



Design of Merensky Reef crush pillars

by B.P. Watson*, J.S. Kuijpers†, and T.R. Stacey‡

Synopsis

The Bushveld platinum group metal deposits are two distinct, shallow-dipping stratiform tabular orebodies which strike for many hundreds of kilometres. Mining is extensive, with depths ranging from close-to-surface to 2 300 m. The mining method is a variation of planar open stoping. Pillars are widely employed to support the open stopes. In the deeper levels, in-stope pillars are required to fail in a stable manner soon after being cut, and the residual pillar strength is used to stabilize the hangingwall. These pillars are commonly known as crush pillars. Little work has been done in the past to determine pillar peak and residual strengths, and pillars have been designed using experience and formulae developed for other hard-rock mines. This has led to over and undersize pillars with consequential loss of ore, pillar bursts and potential collapses. This paper describes a crush pillar design methodology, and provides design charts. Three mining environments were incorporated in the investigations, which included underground and laboratory measurements, analytical solutions, numerical models and back analyses. The results of the study are suitable for the areas where the research was carried out, and may also be applied with caution in other similar environments.

Keywords

Crush pillar design, peak pillar strength, residual pillar strength, *in situ* measurements, design charts.

Introduction

The Bushveld Complex is a large layered igneous intrusion which spans about 350 km from east to west. It is situated in the northern part of South Africa (Figure 1). The platinum group metals are concentrated in two planar orebodies known as the Merensky Reef, a mineralized pegmatoidal pyroxenite 0.7 m to 1.4 m thick, and, underlying this, the UG2 Reef comprising one or more chromitite seams of similar thickness.

The strata generally dip at 8° to 15° toward the centre of the complex. The horizontal to vertical stress ratio (*k* ratio) varies from about 0.5 to over 2.5. The depth of mining ranges from outcrop to 2 300 m.

If a sufficiently large mining span is achieved, or the stope abuts a geological feature, a large volume of hangingwall rock can become unstable, resulting in a stope collapse, or colloquially, a 'backbreak'¹. In order to prevent these backbreaks a high resistance support system is required. This is universally achieved by the use of small in-stope chain pillars orientated either on strike for breast mining (Figure 2) or on dip for up- or down-dip mining.

In the past, pillars on the Merensky and UG2 reefs have been designed using experience and peak strength formulae derived for other hard-rock mines. The consequence of this uncertain methodology is to cut oversize pillars, which lowers the extraction ratio. In addition, pillars cut in the deeper levels are required to fail in a stable manner soon after being cut. These pillars are known as crush pillars and their residual strengths provide the required support resistance to prevent backbreaks and keep the stope hangingwall stable. A recent series of pillar bursts, with serious consequences, has raised questions about the design of these pillars.

The main objective in 'crush' pillar design is to ensure that the residual strength of the 'crush' pillars is sufficient to arrest a backbreak. Pillar size should therefore be designed with the residual strength in mind. However, the pillar bursts show that the peak strength and loading environment also need to be considered in the design.

In the Bushveld platinum mines, the residual strength criterion is 1 MPa across the stope (Roberts *et al.*²). This is achieved if the residual strengths of pillars are between 8 MPa and 13 MPa and the pillar lines are spaced 30 m apart.

* Goldfields Ltd and University of the Witwatersrand, Johannesburg, South Africa.

† CSIR, Johannesburg, South Africa.

‡ University of the Witwatersrand, Johannesburg, South Africa.

© The Southern African Institute of Mining and Metallurgy, 2010. SA ISSN 0038-223X/3.00 + 0.00. Paper received Jul. 2010; revised paper received Sep. 2010.

Design of Merensky Reef crush pillars

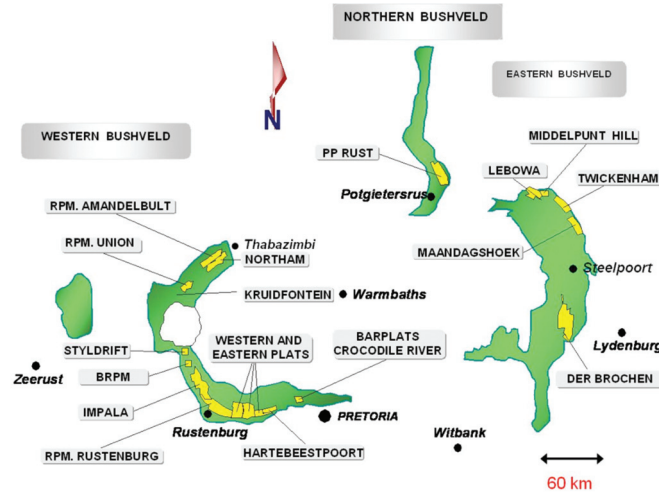


Figure 1—The extent of the Bushveld platinum exposure

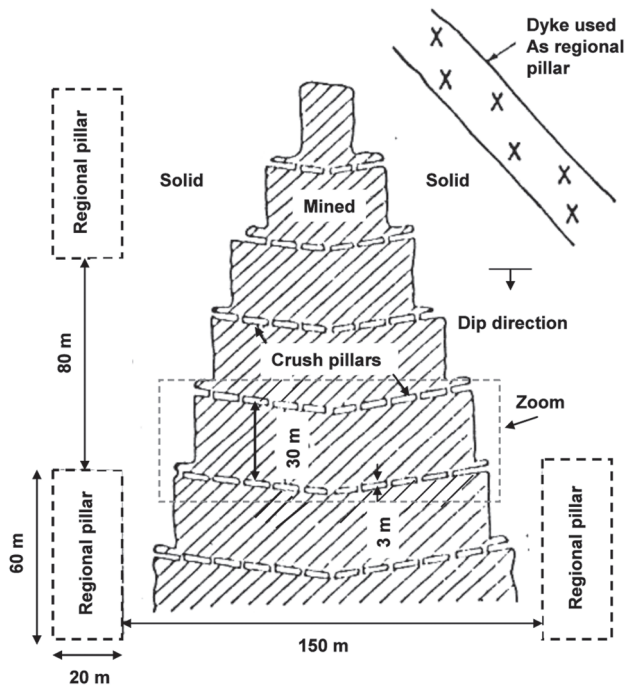


Figure 2—Plan view of a typical stope on one of the platinum orebodies

The aim of the research described in this paper is to provide a crush pillar design methodology, based on solid rock mechanics and backed by underground and laboratory measurements. The investigations were conducted on the Merensky Reef at the Impala Platinum Mine, and in the Thabazimbi and Kruidfontein areas. Therefore the results described in the paper are applicable to the Merensky Reef, but the concepts may be used in any crush pillar design. It is recommended that separate measurements of loading stiffness and pillar strength be made for other environments.

Peak pillar strength

An empirical formula for determining peak pillar strength of Merensky pillars was determined by Watson *et al.*³ for pillars

at the Impala Platinum Mine. This formula, Equation [1], shows a linear relationship between pillar size and peak strength.

$$Strength = 136 \left[\frac{1.27}{1 + \frac{0.27w}{L}} \right] \left[0.59 + 0.41 \frac{w}{h_e} \right] \quad [1]$$

where: h_e accounts for the influence of a gully cut adjacent to one side of the pillar. This influence was determined by Roberts *et al.*⁷:

$$h_e \approx [1 + 0.2692(w/h)^{0.08}]h \quad [2]$$

w and h are the pillar width and mining height, respectively, and L refers to the pillar length.

Merensky pillar behaviour, including peak and residual strength, was measured on six pillars of variable size from three different mines. The results of these measurements are discussed in detail in Watson⁴, and the peak strengths are compared to Equation [1] in Figure 3.

A good fit was shown by all the monitored pillars except by the two highlighted pillars from the Thabazimbi area, which are underestimated by the formula. Interestingly there appears to be less foundation damage in this area than in the

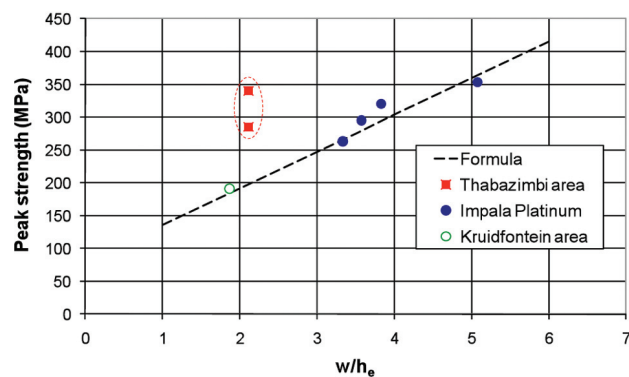


Figure 3—Comparison between the formula and measurements of peak pillar strength

Design of Merensky Reef crush pillars

other areas. The generally good correlation of the measured data with the formula strengthens the applicability of the linear Watson *et al.*³ equation to the calculation of peak pillar strength, particularly at the Impala site and in the Kruidfontein area.

Strata stiffness

Pillars that are properly designed should fail stably near the face where the loading environment is stiff. However, pillars that are too large may fail in a violent manner, away from the face where the loading conditions are softer. Three pillar bursts were investigated to provide some insights into acceptable and unacceptable loading stiffnesses for Merensky pillars. All the pillar bursts occurred on the first or second fully formed pillar back from the lagging face. The pillar distances were thus greater than 10 m back from the lagging face, as shown in Figure 4. One of these bursts created a magnitude 1.2 seismic event, resulting in violent ejection of rock as shown in Figure 5. This pillar was located between 10 m and 14 m behind the lagging face at the time of the burst (Figure 4). A high degree of fragmentation was observed throughout the pillar and rock fragments were thrown into the ASG.

Most of the instrumented pillars failed in line with, or just behind, the lagging face. Only two pillars failed as stubs about 4 m to 5 m behind the face, as shown in Figure 6. Pillar P0 failed in a semi-stable manner at about 7 m behind the lagging face (Figure 7). As all the pillars failed stably with only a minor ejection of rock from one of the pillars, loading conditions at 5 m to 7 m from the lagging face appear stiff enough. However, evidence from the pillar bursts suggests that unfailed pillars located at 10 m or more from the face are in a dangerous, soft-loading situation and may burst if failure takes place.

From the evidence of the few collapses referred to above, surrounding strata stiffness for acceptable and unacceptable loading conditions have been determined from elastic modelling (Figure 8). The elastic acceptable deformation in the figure is based on the average deformation across the area of the pillar at a face advance of 4 m (Figure 6). The underground line in Figure 8 refers to deformation measurements which can practically be conducted

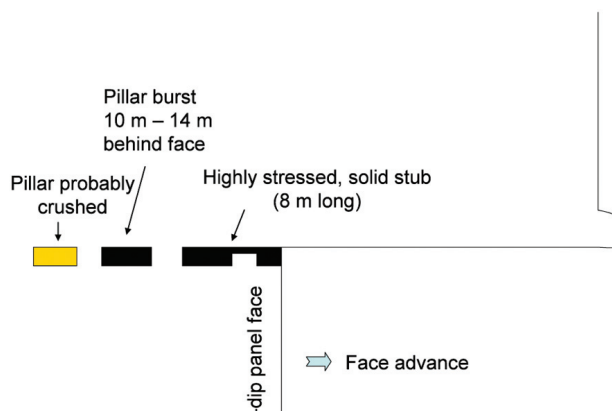


Figure 4—Plan view showing the face position where the investigated pillar bursts occurred (not drawn to scale)



Figure 5—Panoramic view showing the up-dip end of a burst pillar. Note the gully is full of rock fragments from the pillar burst

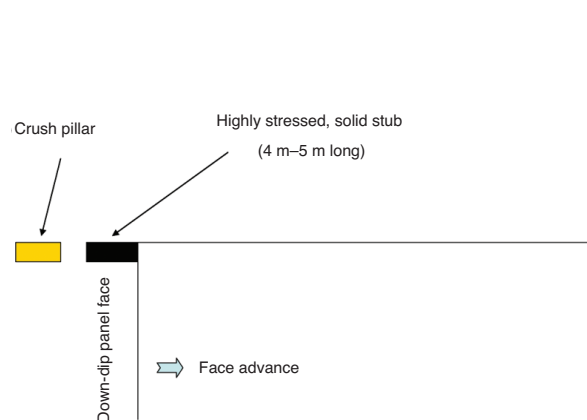


Figure 6—Plan view showing the face position where two of the monitored pillars failed (not drawn to scale)

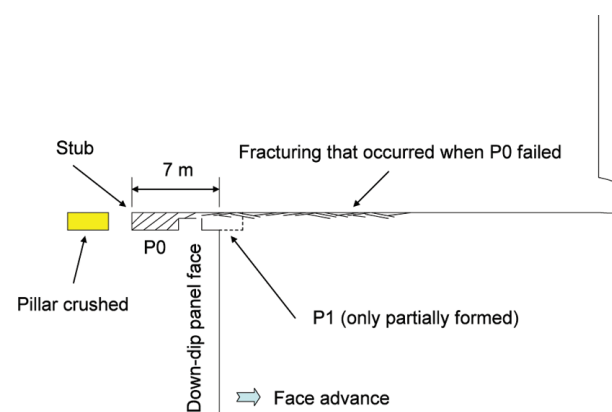


Figure 7—Sketch showing the fracturing that occurred when P0 failed

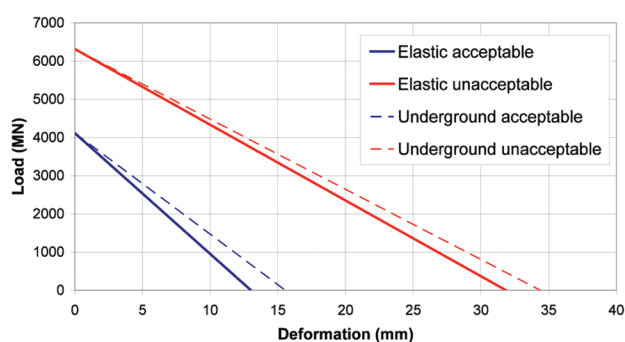


Figure 8—Acceptable and unacceptable stiffness of the surrounding strata for stable 'crush' pillar design. Elastic = average deformation over pillar, underground = deformation measured adjacent to pillar

Design of Merensky Reef crush pillars

underground. These measurements should be conducted about 2 m on the down-dip side of the pillar edge and at about the mid-point of the pillar. In the model, the surrounding pillars were assumed to have a residual strength of 20 MPa.

The unacceptable loading conditions refer to the same scenario as the acceptable model but for conditions where the pillar fails at 8 m to 10 m behind the face. Most of the measured pillar load-deformation curves were almost parallel to the elastic acceptable line. None of the instrumented pillars reached a deformation of 32 mm during the initial failure and all failed in a reasonably stable manner. The unacceptable stiffness of the surrounding strata is about 5.0 mm/GN. Most of the measured pillars failed under loading conditions where the stiffness of the surrounding strata was about 3.2 mm/GN

Residual pillar strength

The residual strength of pillars was determined using field-stress and stress-change measurements conducted relatively high (4 m–6 m) above the pillars. These measurements were confirmed by a series of field measurements conducted at regular intervals just above each pillar. The pillar stress profile and average pillar stress (APS_r) were extrapolated from the series of measurements using an inverse matrix of Boussinesq equations:

$$\sigma_{zz} = \sum_{i=1}^n \left[\frac{3A_i}{2\pi} \times \frac{z_i^3}{(x_i^2 + y_i^2 + z_i^2)^{3/2}} p_{zi} \right] \quad [3]$$

where:

σ_{zz} = stress at a point in space

A_i = Area of the grid 'i'

p_{zi} = Vertical stress carried by the grid 'i'.

A plan view of a typical Boussinesq co-ordinate system used across the top boundary of a pillar is shown in Figure 9. The grid enabled multiple stresses to be considered across the pillar.

Laboratory tests

Laboratory tests were conducted by Spencer and York⁵, using a cylindrical punch 'pillar' of 25 mm diameter and a foundation cylinder of 80 mm for both the diameter and the length. The foundation was confined by a metal ring. Both the punch and the foundation were anorthositic norite from the immediate Merensky Reef footwall at Impala Platinum. This material is typical of the lower half of the pillars and immediate footwall of the Merensky Reef at that mine.

The w/h ratio of the punch was varied by changing the punch height. The boundary condition at the top of the punch controls the effective w/h ratio. Should the interface between the punch and the metal platen have been frictionless, the w/h ratio would have been halved as this interface acts as an axis of symmetry (absence of shear stress). Since this interface had a friction angle of about 12° (York and Canbulat⁶), it could neither be regarded as a plane of symmetry nor a rough interface similar to the one between the punch and the foundation. The true w/h ratio will therefore be greater than 50% of the actual w/h ratio of the punch, but the effective ratio cannot be quantified with any certainty. This issue was considered during the analysis of

the results. The peak strengths of the laboratory tests (Figure 10) were similar to the strengths provided by the linear peak strength formula.

The initially higher rate of increase of peak strength with w/h ratio in Figure 10 was also shown by FLAC⁷ modelling (Watson *et al.*⁵). However, there was a drop in the rate of strength increase at the highest w/h ratio in the laboratory test, indicating pillar punching (assuming: the punches; foundations; and confinements provided to the foundations by the metal rings were the same in all three tests).

The results of the pillar residual strength measurements are plotted with the Spencer and York⁵ laboratory tests in Figure 11. At low w/h ratios there was good agreement between the underground measurements and the laboratory results. However, at larger w/h ratios the discrepancy was great. This observation will be discussed further on.

Analytical analysis of residual strength

If it is assumed that a pillar consists of small vertical slices that are subjected to a uniform stress, it is possible to obtain a limit equilibrium solution for a perfectly plastic material

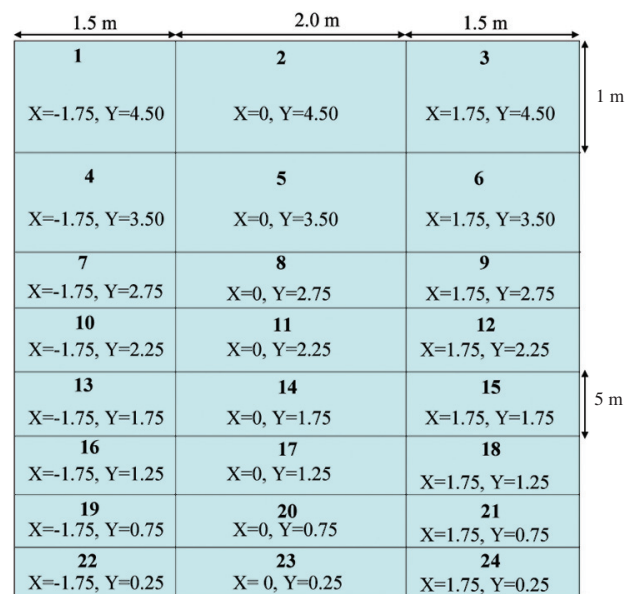


Figure 9—Plan view of the grid layout across a pillar for a Boussinesq evaluation. The origin is the centre of the bottom (down-dip edge)

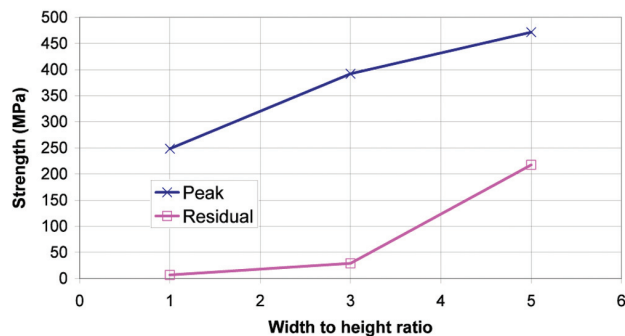


Figure 10—Results of laboratory punch tests (after Spencer and York⁵)

Design of Merensky Reef crush pillars

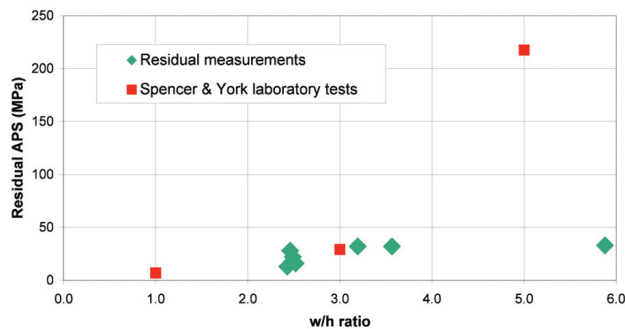


Figure 11—Residual strength results

that is yielding. According to Barron⁸, the vertical stress distribution through a pillar, consisting of such a material, can be expressed as:

$$S_{yy} = \frac{UCS_b}{2 \sin \phi_b} \left\{ (1 + \sin \phi_b) e^{\tan \phi_b \left(\frac{1 + \sin \phi_b}{1 - \sin \phi_b} \right) \frac{x}{h}} - (1 - \sin \phi_b) \right\} \quad [4]$$

where:

- S_{yy} = Vertical stress within the pillar
- ϕ_b = Internal friction angle of the broken rock
- UCS_b = Uniaxial compressive strength of the crushed (broken) material
- x = Horizontal distance into the pillar
- h = Pillar half height.

Figure 12 illustrates the pillar geometry, as well as the stresses acting on a vertical slice. The pillar width and height equal $2w$ and $2h$ respectively.

Equation [4] shows that the residual strength of a pillar with a given w/h ratio is dependent on the uniaxial strength (UCS_b) and internal friction angle (ϕ_b) of the broken rock. Assuming a constant ϕ_b , the pillar residual strength would be directly related to the UCS_b . The UCS_b is, in turn, dependent on the residual cohesion (C_b) and the ϕ_b (Mohr-Coulomb criterion):

$$UCS_b = \frac{2C_b \cos \phi_b}{1 - \sin \phi_b} \quad [5]$$

Therefore, the residual cohesion is extremely relevant to the behaviour of a failed pillar. In addition, any horizontal stress applied at the pillar edge, e.g. support, has a similar effect. The residual cohesion can be thought of as a frictional effect due to gravity, which leads to small values in the kPa range. There may also be additional residual strength associated with interlocking of rough fracture surfaces. An equivalent residual cohesion (C_b) of 0.011 MPa was estimated from the effects of gravity on a pile of rock at the edge of a pillar. Assuming $UCS_b = 0.038$ MPa, which relates to $C_b = 0.011$ MPa, and $\phi_b = 30^\circ$, the Barron⁸ pillar stress was plotted as a function of distance across the pillar and is shown in Figure 13. The results were also compared to the measured vertical stress profile of a pillar measured in the Thabazimbi area, 'P1' in the figure. The analytical solution provided a much smaller profile than P1 and it was necessary to increase the UCS_b to 0.7 MPa to provide a comparable profile (Figure 13). Assuming $\phi_b = 30^\circ$, a C_b of 0.2 MPa was calculated from Equation [5]. The analytical solution

suggests an exponential increase in vertical stress near the edge of the pillar. However, an almost linear stress increase was generally interpolated from the measurements (Figure 13).

Equation [4] was integrated to obtain the APS:

$$APS_r = \frac{h}{w} \left[\frac{UCS_b}{2 \sin \phi_b} \left\{ \left(\frac{1 - \sin \phi_b}{\tan \phi_b} \right) \frac{x}{h} \right\}^{\tan \phi_b \left(\frac{1 + \sin \phi_b}{1 - \sin \phi_b} \right)} - (1 - \sin \phi_b) x \right] \quad [6]$$

Using the same parameters as determined for the curves in Figure 13, Equation [6] was plotted against w/h ratio and compared to the residual strengths measured underground (Figure 14). The residual strengths measured in a laboratory by Spencer and York⁵ in their punch tests, are also included in the figure. The solution that provided a reasonable fit to P1 in Figure 13 ($C_b = 0.2$ MPa) does not fit the laboratory data and appears to overestimate residual strength at w/h ratios exceeding about 3. The solution for $C_b = 0.011$ MPa appears to underestimate the residual strengths even at comparatively high w/h ratios and does not compare with either the underground or laboratory results. However, both the Barron⁸ solutions and the laboratory results show an exponential increase in residual strength with w/h ratio. The exponent in the relationship shown by the laboratory tests in Figure 14, suggests a friction angle of $\phi_b = 30^\circ$.

Salamon⁹ derived relatively complicated expressions to describe the stress distribution in a plastic pillar, that allow for a non-uniform stress distribution in the vertical slices (Equation [7]). This equation is more realistic than the Barron⁸ solution.

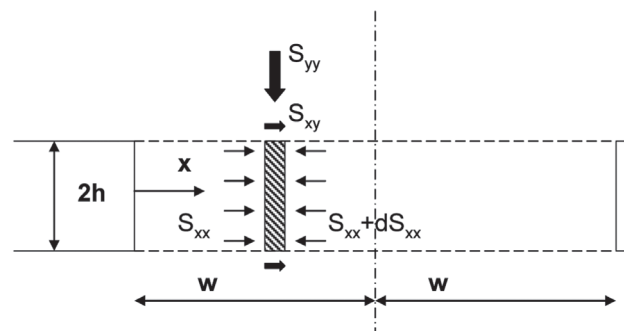


Figure 12—Geometry of the pillar section assumed in Equation [4]

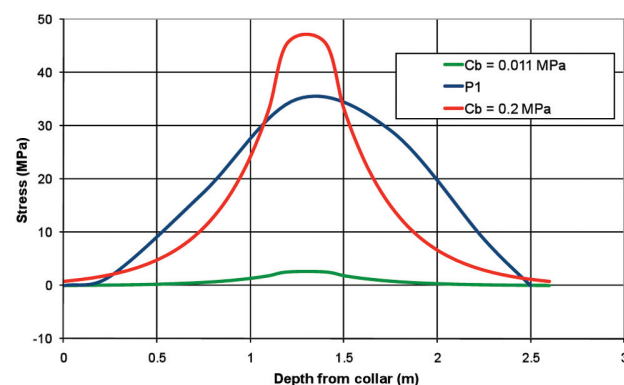


Figure 13—Comparison between the Barron⁸ formula and the P1 stress profile. Assuming $\phi_b = 30^\circ$ in the formula. 2.5 m-wide pillar in a stoping width of 1.1 m

Design of Merensky Reef crush pillars

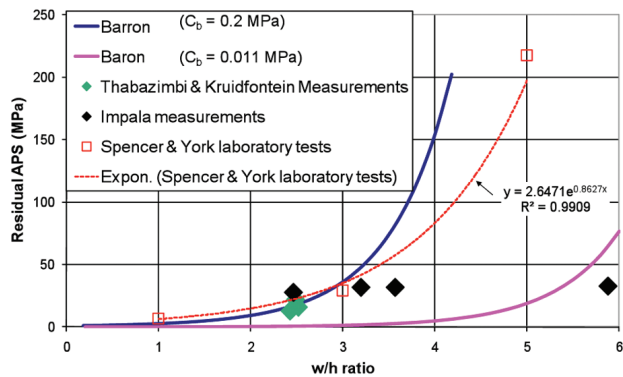


Figure 14—Pillar w/h ratio-strengthening effects on APS_r. The Barron⁸ solutions for $\phi_b = 30^\circ$ are compared to the measurements and the Spencer and York⁵ laboratory tests

$$APS_p = \frac{2h \times 0.8 \frac{C_b}{0.5} \left[e^{2.5\left(\frac{w}{2h}\right)} - 1 \right]}{2.5w} \quad [7]$$

The curves for cohesions of 0.011 and 1.6 are plotted in Figure 15. For completeness the laboratory residual strengths (Spencer and York⁵) are also included in the figure.

It should be emphasized that there are differences between laboratory tests and analytical solutions. For instance, the analytical solution is based on the limit equilibrium of the material that is loaded between two solid platens; in contrast, the punch test allows for damage in the foundation. This foundation damage can have serious implications for peak pillar strength as has been demonstrated in Watson *et al.*³. It is very plausible that residual strength is also affected by foundation damage. In addition, the formulae are based on plane strain conditions, whereas the laboratory tests were axisymmetrical. This geometric effect will also result in different relationships between w/h ratio and strength.

Despite the differences, an attempt was made to match the laboratory results with the Salamon⁹ analytical model (Equation [7]). Since the Salamon⁹ equation does not account for foundation damage, there is an overestimation of the stress around the core of the pillar. Thus the APS_r may also be overestimated. This would be particularly true for larger w/h ratios.

It can also be argued that the w/h ratio of the laboratory specimens was affected by the boundary conditions, especially the interface between the steel platen and the small rock disc. The limited friction along this interface would cause a decrease in the effective w/h ratio of the disc because of a reduced clamping effect. If it is assumed that this decrease could be as much as 25%, the parameters for the Salamon⁹ equation (Equation [7]) need to be adjusted. A sensitivity analysis showed that the friction angle and the residual cohesion could vary between 25° and 31° and 0.7 MPa and 1.6 MPa, respectively, to match the laboratory results with the equation.

The Salamon⁹ curve with a residual cohesion of 1.6 MPa (Figure 15) fitted the underground measurements from the Thabazimbi and Kruidfontein areas as well as the laboratory tests (Spencer and York⁵). However, the underground data is

clustered within a very small range of w/h ratios. Therefore, the suitability of the equation for describing the pillar residual strength at these sites may be questionable.

The Salamon⁹ equation for stress distribution across the centre of a pillar (h) was applied, assuming $\phi_b = 30^\circ$ and a cohesion of 1.6 MPa in Equation [8].

$$S_{yy} = 3.2 \left(0.8 \times e^{\left(\frac{2.5x}{2h}\right)} \right) \quad [8]$$

The analytical solution was compared to the stress profile determined for P1 in Figure 16. It should be noted that neither the Barron⁸ nor the Salamon⁹ equation considers the effects of the foundations on pillar behaviour; i.e. the foundations are considered to be elastic and the interface friction between the pillar and the loading platen is assumed to be equal to the internal friction of the material. Thus the equations predict 'squat' pillar behaviour, which was not observed underground. In the analytical solution, a high w/h ratio would be associated with vertical stresses that are beyond the punching resistance of the foundation (hangingwall or footwall). This is an explanation why the larger pillar w/h ratios may not be well represented by the analytical solutions shown in Figure 15.

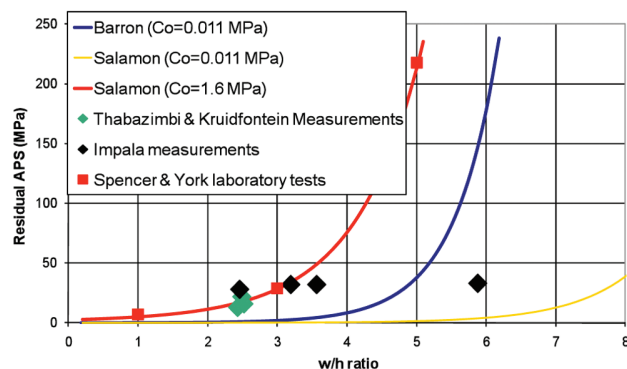


Figure 15—Pillar w/h ratio-strengthening effects on APS_r. The measurements are compared to the Barron⁸ and Salamon⁹ solutions ($\phi_b = 30^\circ$), and the Spencer and York⁵ laboratory tests

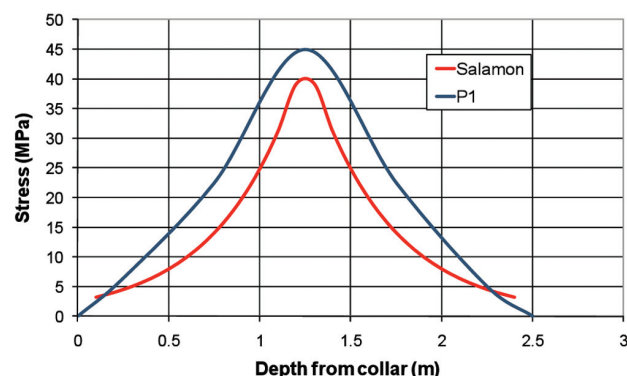


Figure 16—Comparison between the Salamon⁹ formula (Equation [8]), assuming $\phi_b = 30^\circ$ and Co = 1.6, and the measured P1 stress profile

Design of Merensky Reef crush pillars

Flac modelling

A series of FLAC7 models were constructed to investigate pillar behaviour in the context of a realistic loading environment. This environment included the pillar foundations that could sustain damage. For the purposes of the model, the foundation material properties were assumed to be the same as the pillar, which was a reasonable approximation for the pillars at all three sites. The model included the pillar itself and the immediate hanging- and footwalls.

One important parameter that needed to be considered for pillar behaviour was material brittleness. In the models, brittleness is defined as the rate of stress decrease after failure. In these models, post failure behaviour is controlled by cohesion softening. Therefore, a direct relation between cohesion softening (strain softening) and material brittleness can be quantified. The internal friction angle and the dilation angle were not varied in these models to avoid additional complications.

In the numerical models brittleness is unfortunately also affected by grid size, since it influences failure localization. Therefore the model brittleness is controlled by both the post failure strain softening and the grid size. This issue was considered in the model analyses. While brittleness does not affect the strength of typical slender uniaxial and triaxial test specimens, it becomes very relevant in (pillar) geometries with larger w/h ratios. In the larger w/h ratio geometries, failure progresses from the edge towards the core of the pillar even before the peak pillar strength is reached. In the case of a comparatively brittle material, the failed material will rapidly lose its strength and failure can progress relatively easily into the pillar. Failure initiation and peak strength will be of similar magnitude. However, a more ductile material will maintain some strength after failure and failure progression into the pillar will be retarded. The core of the pillar will be confined by the partially failed material and is able to sustain a higher load. As a consequence the magnitude of failure initiation will be much lower than the peak strength.

Figure 17 shows the Mohr-Coulomb parameters that were used in the model. These parameters were calibrated from underground measurements of pillar stress and strain and laboratory results.

Boundary conditions play an important role in the punching mechanism, as they affect horizontal confinement. In the models (Figure 18), the vertical boundaries were not allowed to move in a horizontal direction (thus simulating a fully replicated set of pillars). The presence of discontinuities such as bedding planes, faults and joints should also affect the punch resistance, but this was not investigated in the models. While the numerical models provide insight into the failure mechanisms, it must be emphasized that these models always need to be calibrated against realistic data. Mesh density and rate of softening are important parameters in this respect and they cannot be arbitrarily selected.

The models were used to evaluate the peak pillar strength formula derived from the back-analysis. The stope span was about five times the pillar width (extraction ratio ~ 83%) and the model height was more than eight times the pillar width. The model results are compared to the peak pillar strength formula and the peak strengths of the Spencer and York⁵

laboratory tests in Figure 19. The strengths shown in the figure were slightly higher than measured at the instrumentation sites, due to the 2D conditions assumed in the model. These 2D conditions were accounted for by assuming infinitely long pillars in the equations. In the laboratory tests, the boundary condition at the top of the punch was unrealistic and this parameter controls the effective w/h ratio. In addition, the shape of the pillar was different to the normal underground pillars and the ratio in size between the punch and foundation did not adequately represent the underground situation. Despite these differences, a remarkable comparison is shown in Figure 19. The numerical modelling showed a levelling off of peak strengths for w/h ratios in excess of eight. This levelling off is associated with full punching into the surrounding strata.

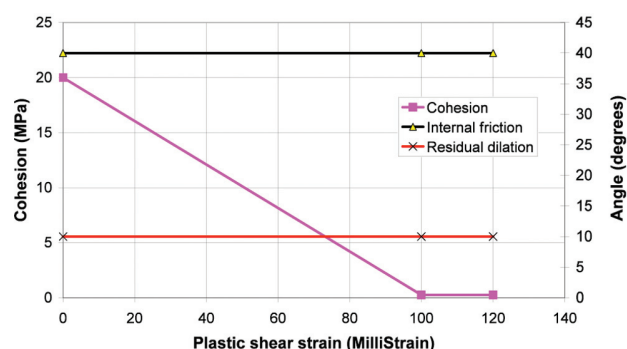


Figure 17—FLAC7 model properties

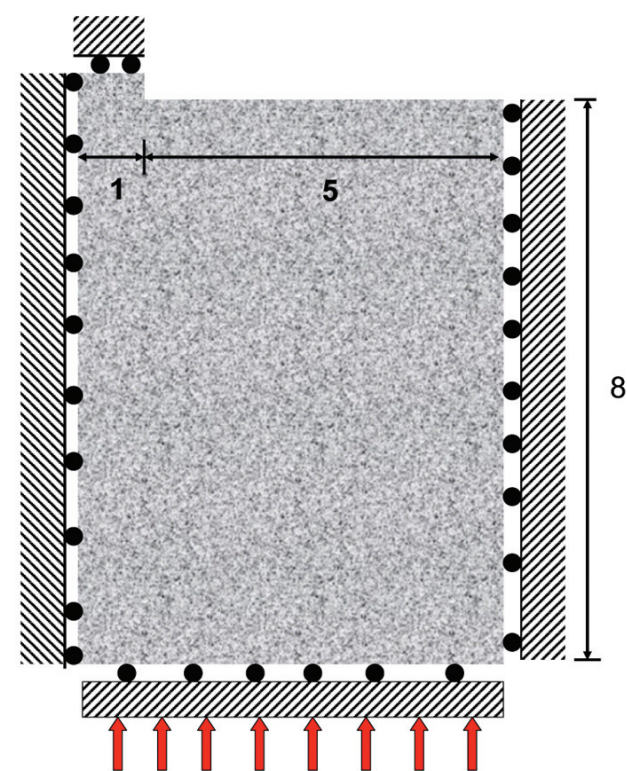


Figure 18—Diagram showing the double symmetry FLAC7 model used in the pillar and foundation investigations. The model was loaded along the bottom edge

Design of Merensky Reef crush pillars

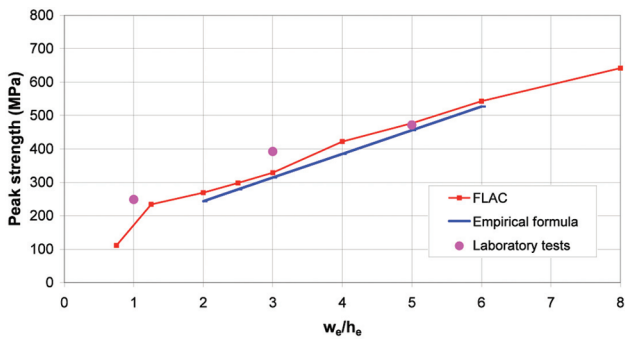


Figure 19—Comparison between the strength database, FLAC7 modelling and laboratory tests performed by Spencer and York⁵

The models were continued into post failure to observe the residual strength of the pillars. A significant drop in stress occurred when the loading rate was reduced to zero, indicating some form of ‘plastic’ flow resistance associated with the loading velocity. Obviously, this factor needs to be excluded to obtain more realistic results. The subsequent very slow loading rate did not change the residual strength achieved during the zero velocity loading. It was therefore assumed that these residual strengths were not influenced by the flow resistance issue.

The models showed that there is an almost linear increase in residual strength with w/h ratio up to a w/h ratio of about 3 (Figure 20). Although the models appear to have reached the bearing capacity of the foundations at a w/h ratio of 3, the peak strength increased with w/h ratio, to a w/h ratio of about 10. A good match between the underground results, the two lower w/h ratio laboratory tests and the FLAC⁷ models was shown when a cohesion of 0.26 was assumed in the model. This was achieved even with a constant friction angle of 40° for the peak and residual strength. A sensitivity analysis on the effect of the friction angle and cohesion on residual strength is described in Section 8.

The larger w/h ratios may not be well represented by the Salamon⁹ solution because it predicts ‘squat’ pillar behaviour, which was not observed underground.

The ultimate bearing capacity of the pillar foundation is dependent the cohesion and friction and dilation angles of the foundation material. No further increase in residual pillar strength can thus be expected above the bearing capacity. The results in Figure 20 suggest that the effective range of w/h ratios is limited to a maximum of about three. No further increase in strength can be expected for greater w/h ratios.

Foundation bearing capacity

Neither the analytical nor the laboratory results matched the linear relationship between pillar residual strength and w/h ratio as measured underground at the Impala site (Figure 15). Since the pillars at this site represent mainly the higher w/h ratios, the almost zero increase in residual strength with w/h ratio was suspected to be related to bearing capacity. The effects of the fractured foundation were therefore investigated using an analytical solution for bearing capacity.

The relationship between C_b and bearing capacity (BC) for a given friction angle is shown in Equation [9] (Meyerhof¹⁰). The dilation and friction angles are assumed to be the same in the equation (associative flow rule).

$$BC = \left[\left(e^{\pi \tan \phi} \tan^2 \left(45 + \frac{\phi}{2} \right) - 1 \right) \cot \phi \right] \times C_0 \quad [9]$$

Bearing capacity has been plotted as a function of cohesion for friction angles of 30° and 40° in Figure 21. The ultimate bearing capacity of the pillars as shown in Figure 20 appears to be about 33 MPa. This suggests cohesions of about 1.1 MPa or 0.4 MPa for friction angles of 30° or 40°, respectively. The FLAC⁷ models indicated a cohesion of 0.3 MPa at a friction angle of 40°. The small difference between the model and the analytical solution is probably because the associative flow rule was not assumed in the model. The dilation angle in the model was 10°.

The good agreement between the Salamon⁹ solution and the residual strength from the laboratory results as given in Figure 20, suggests that pillar punching either did not occur or was restricted in the laboratory tests. This was probably true for the two smaller w/h ratios as there is reasonable correlation between the laboratory, underground and FLAC⁷ results. However, the residual strength of the rock punch with a w/h ratio of 5 was significantly higher than the other results even though there was a good match with the peak strength and the underground results. The peak results from the laboratory tests appear to suggest punching, whereas the residual laboratory test results suggest that punching is not occurring. This apparent contradiction can be explained in several ways:

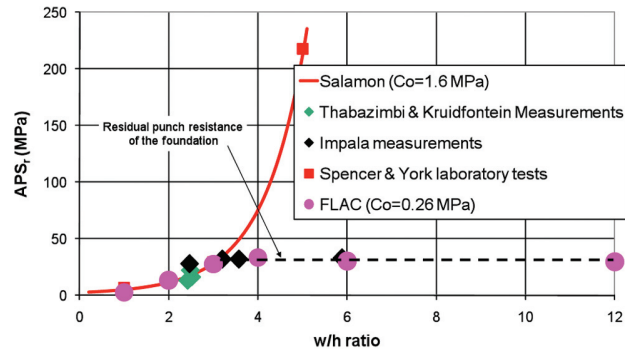


Figure 20—Pillar w/h ratio-strengthening effects on APS_r . The FLAC⁷ models ($\phi_b = 40^\circ$) are compared to the Salamon⁹ equation ($\phi_b = 30^\circ$), Spencer and York⁵ laboratory results and the underground measurements

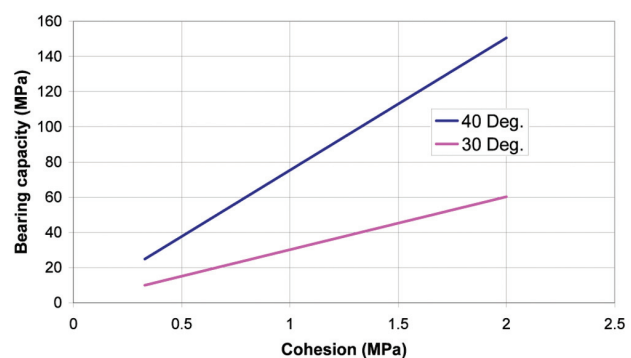


Figure 21—Ultimate bearing capacity of the foundation, assuming friction angles of 30° and 40°

Design of Merensky Reef crush pillars

- Relatively large post-failure punch dilations, in the high w/h ratio sample, resulted in stress being generated in the dilated fractured sidewall between the metal loading platen and a solid foundation
- Interference of the boundary on the results (the foundation cylinder was only three times larger than the solid punch) and
- The grain size is large in comparison to the height of the punch. Post-failure behaviour may therefore have been influenced by fractures developing through relatively strong grains.

It is strongly recommended that this phenomenon is researched further by appropriate laboratory tests.

Post-failure cohesion

The cohesion suggested by the analytical solutions and the modelling is much higher than would be expected of a crushed material. One possible explanation is that the material is not completely crushed and that the broken rock actually maintains a surprisingly high residual strength. The pillar centre may also be comparatively more ductile and therefore less fractured as a result of confining stresses that could develop here. The effect of confinement on brittleness was researched by Fang and Harrison¹¹. The residual strength resulting from friction between blocks, held together by gravity, would only account for about 1% of the calibrated value. The relatively high strength of broken rock has not been reported previously but it is an extremely important parameter, especially for the design and behaviour of 'crush' pillars. Factors influencing the residual strength may be: interlocking blocks, block size, failure violence, peak strength and residual cohesion. These factors may not be constant.

The uncertainty of the relatively high residual cohesion-mechanism is of concern as adequate residual strength may not always be present. This inadequate residual strength was also suggested by the stress drop that occurred after mining had been completed in a stope in the Kruidfontein area (Figure 22).

Further investigations are required to determine the reasons for the generally high post-failure cohesion required to simulate the residual pillar strengths measured underground. This may include the development of a more appropriate post-failure strength criterion.

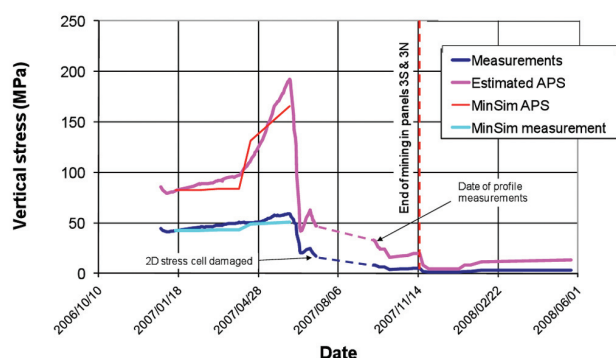


Figure 22—Kruidfontein area: vertical stress measurements and estimated P1 APS and the results of an elastic MinSim model

Design strategy

The pillar investigations suggest a direct relationship between peak pillar strength and w/h ratio up to a w/h ratio of about 8. Larger pillars are thus less likely to fail near the face than smaller pillars. Pillar strength should not exceed the available loading capacity of the system within 5 m to 7 m of the face. At shallow depths this would require very slender pillars that may not have sufficient residual strength to stop a backbreak. Under these conditions pillar preconditioning could be an option. A flowchart for the design of 'crush' pillars is provided in Figure 23. The process assumes that a suitable residual strength is calculated on the basis of strength requirements. The approximate pillar w/h ratio to provide the strength requirements can be determined from Figure 24. The calculations should include panel spans between pillars rather than a pure extraction ratio. An elastic model should be run to determine if the loading capacity is sufficient to fail the required pillar within 5 m of the face. It should be pointed out that the peak pillar strength calculated using Equation [1], and reproduced in Equation [10], provides a 50% probability of failure.

$$Strength = 136 \left[\frac{1.27}{1 + \frac{0.27w}{L}} \right] \left[0.59 + 0.41 \frac{w}{h_e} \right] \quad [10]$$

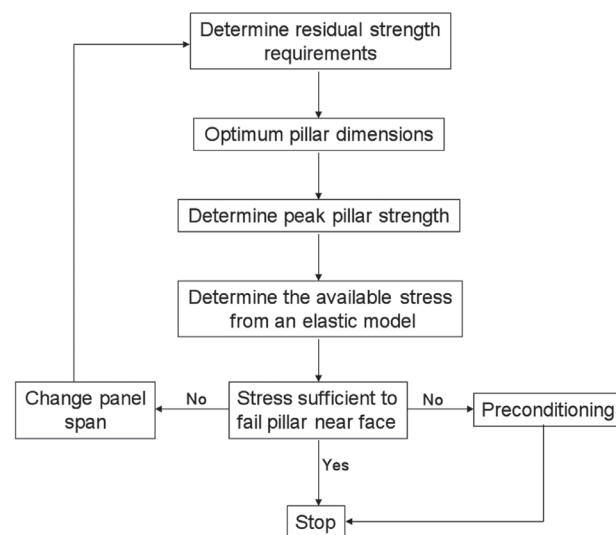


Figure 23—Flow chart for 'crush' pillar design

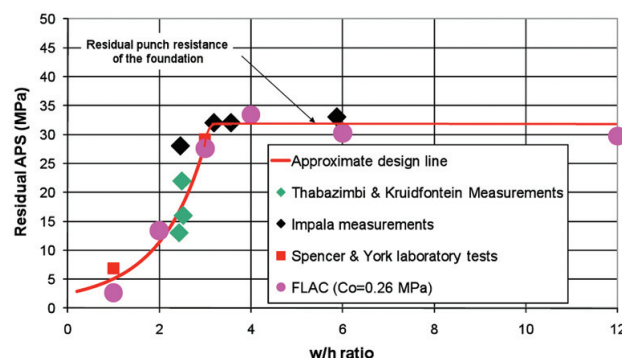


Figure 24—Pillar residual strength as a function of w/h ratio

Design of Merensky Reef crush pillars

The probability of failure can, however, be increased by ensuring a greater available loading capacity than calculated by the equation. Figure 25 shows the stresses that should be added to the results of Equation [10] to provide the desired probability of failure for three pillar w/h ratios.

Should the loading capacity be insufficient to fail the pillars, either preconditioning or redesign of panel spans must be considered. Smaller spans will require smaller residual strengths and thus smaller pillars. The elastic model and process shown in the flow chart (Figure 23) should be repeated with the new layout. 'Crush' pillars located adjacent to stability pillars or potholes (left as stability pillars) may need to be cut smaller than other pillars in a panel to ensure adequate loading conditions.

The stoping width affects the pillar height and is often variable across a panel. For this reason pillars cut to size may have different residual strengths resulting from the stoping width adjacent to the pillar. The issue of stoping width is of particular interest when the margin between the required and supplied residual strength is small. The relationship between stoping width and pillar residual strength is provided in Figure 26. The relationship is based on the parameters shown in Figure 24, assuming a standard 3 m-wide pillar. Pillar cutting is difficult and some mines struggle to cut standard sized pillars. An analysis of residual strength versus pillar-width variability in a stoping width of 1.2 m is provided in Figure 27.

Conclusions

Three factors need to be considered during the design of a crush pillar:

- Residual strength requirements;
- Loading stiffness of the environment, and how this varies with distance from the face; and
- The relationship between peak pillar strength and w/h ratio.

The parameters for Merensky pillars have been researched for three different mining environments. Design charts have been developed from the investigations and these are presented in the paper. The results of the research are also discussed.

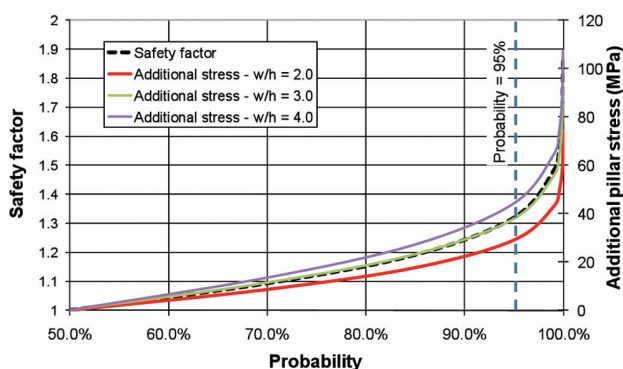


Figure 25—Comparison between the safety factor and the associated additional pillar stress requirements for pillars of w/h = 2.0, 3.0 and 4.0, based on the linear back-fit analysis ($\log s = 0.073$)

A previously formulated peak pillar strength equation for Merensky pillars at the Impala Mine was confirmed by stress measurements conducted at the Impala site and in the Kruidfontein area. Also pillar measurements from the Thabazimbi area were only slightly underestimated by the formula.

Acceptable and unacceptable loading stiffnesses were determined from a back-analysis of stable and unstable pillar failures, respectively. It was found that pillars failing more than 10 m behind the lagging face, could fail violently. However, pillars failing within 5 m to 7 m of this face always failed stably.

The residual pillar strength relationship to w/h ratio was determined by underground stress measurements. It was found that no further strength increase occurred above a w/h ratio of about three. However, limited laboratory tests, in which an attempt was made to reproduce punching, showed an exponential increase up to a w/h ratio of five. This exponential increase in residual strength with w/h ratio was also shown by analytical solutions developed to determine the residual strength of crush pillars. However, these solutions did not include the influence of the foundation on the results, thus predicting squat behaviour that was not observed underground. A FLAC7 model that included the hanging- and footwall simulated the underground measurements and showed that the bearing capacity of the fractured foundations was the controlling factor in the

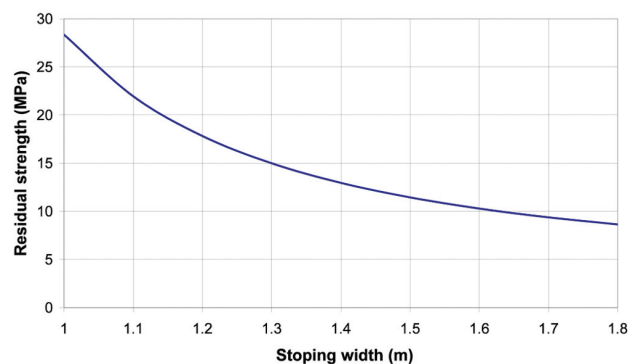


Figure 26—Effect of stoping width on residual strength, assuming a standard 3 m-wide pillar. Salamon⁹ analytical solution with $\Phi_b = 30^\circ$ and $C_o = 1.6$ MPa

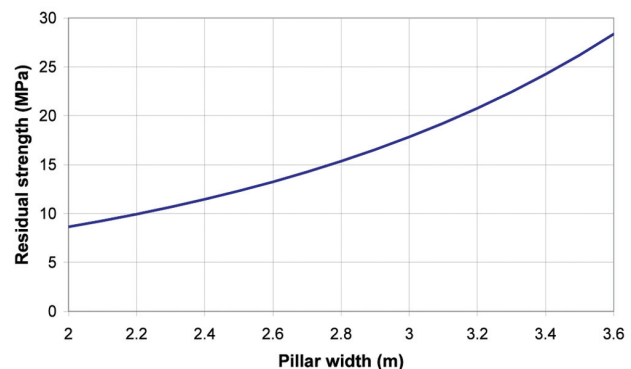


Figure 27—Effect of pillar width on residual strength, assuming a stoping width of 1.2 m. Salamon⁹ analytical solution assuming $\Phi_b = 30^\circ$ and $C_o = 1.6$ MPa

Design of Merensky Reef crush pillars

ultimate residual strength. The model also predicted this ultimate strength from a w/h ratio of three. Both the model and an analytical solution for bearing capacity suggested an unexpectedly high value of cohesion. This important issue needs to be investigated further.

The principles of crush pillar design are universal. However, it is recommended that the results described in this paper be used in the areas where the research was conducted. It is considered that these results may also be cautiously applied in other similar conditions.

Acknowledgements

The CSIR and PlatMine is acknowledged for facilitating the success of the research work described in this paper. In particular, the management and Rock Engineering Departments of Impala Platinum Mine and mines in the Thabazimbi and Kruidfontein areas are thanked for their assistance.

References

- ROBERTS, M.K.C., GRAVE, D.M.H., JAGER, A.J., and KLOKOW, J. Rock Mass Behaviour of the Merensky Reef at Northam Platinum Mine. *Proc. SARES*, Johannesburg, S. Afr. National Inst. For Rock Engng. 1997.
- ROBERTS, D.P., ROBERTS, M.K.C., JAGER, A.J., and COETZER, S. The determination of the residual strength of hard rock crush pillars with a width to height ratio of 2:1, *Jl S.Afr. Inst. Min. Metall.*, vol. 105, 2005. pp. 401–408.
- WATSON, B.P., RYDER, J.A., KATAKA, M.O., KUIJPERS, J.S., and LETEANE, F.P. Merensky pillar strength formulae based on back-analysis of pillar failures at Impala Platinum, *Jl S.Afr. Inst. Min. Metall.*, vol. 108, 2008. pp. 449–461.
- WATSON, B.P. Rock behaviour of the Bushveld Merensky Reef and the design of crush pillars, PhD thesis, School. of Mining Engineering, University of Witwatersrand, Johannesburg, RSA. 2010.
- SPENCER, D and YORK, G. Back-analysis of yielding pillar system behaviour at Impala Platinum Mine, *Proc. SARES99*, Johannesburg, S. Afr. National Inst. For Rock Engng, 1999. pp 44–52.
- YORK, G. and CANBULAT, I. The scale effect, critical rock mass strength and pillar system design, *Jl S.Afr. Inst. Min. Metall.*, vol. 98, no. 1 Jan/Feb, 1998. pp. 27–37.
- ITASCA CONSULTING GROUP, INC. Fast Lagrangian Analysis of Continua (FLAC), Vers. 3.2. Minneapolis Minnesota USA. 1993.
- BARRON, K. An analytical approach to the design of pillars in coal, Contract Report No. 1SQ80-00161, Canada Centre for Mineral and Energy Technology, Energy, Mines and Resources, Canada, 1983. pp. 36–42.
- SALAMON, M.D.G. Strength and stability of coal pillars, Workshop on coal pillar mechanics and design, US Bureau of the Interior, US Bureau of Mines, Santa Fe, USA. 1992.
- MEYERHOF, G.G. The ultimate bearing capacity of foundations, *Geotechnique*, vol. 5, 1951. pp. 301–332.
- FANG, Z. and HARRISON, J.P. Application of a local degradation model to the analysis of brittle fracture of laboratory scale rock specimens under triaxial conditions, *Int. J. of Rock Mech. and Min. Sci.*, vol. 39, 2002. pp. 459–476. ◆

PRETORIA MATRIC LEARNERS SCOOP TOP SCIENCE AWARD*

Pretoria learners emerged as victors of this year's national Minquiz® Science Competition held at Mintek's campus in Randburg on 27 and 28 September 2010. Each member of the winning team walked away with a half-ounce Kruger Rand, sponsored by Rand Refinery Limited and worth about R4 500 each, and their schools received a cash prize of R3 250, sponsored by DCM Deco Metals.

The winners competed against more than 50 other finalists, studying Grade 12 Physical Science and Mathematics at school, who had advanced to the national competition following rigorous provincial competitions in July.

The competition was introduced by Mintek in 1988 with an aim to foster excellence in Mathematics and Physical Science at school and encourage learner interest in careers in Science, Engineering and Technology.

Potchefstroom, North West, were runners-up. Each student in the team received a portable educational microscope from Advanced Laboratory Supplies; each member's school received R2 250 donated by South African entrepreneur, Mark Shuttleworth, a previous Minquiz winner and now a patron of the competition. Sasol, Sasolburg came third; each of its students received a book prize donated by Apollo Scientific and their schools received R1 250 from the Southern African Institute of Mining and Metallurgy (SAIMM).

All the learners in first, second and third positions received a one-year subscription to *Quest*, a science magazine published by the Academy of Science of South Africa. All participants received a certificate of participation, an issue of *Quest*, Grade 12 Physics, Chemistry, Mathematics and languages study guides published by Proverto, and a Sasol encyclopaedia.

Craig Andrews, of Selly Park High School in the North West province, and Antony James Lake, of Fish Hoek High School in the Western Cape, were named top learners in the Platinum and Gold category (written test) respectively. They were each awarded a

Netbook valued at R2 200 and a high-end Texas Instruments scientific calculator worth R2 300, respectively donated by UK-based GFMS and Oxford Educational Supplies.

Heather Elizabeth Rae, of Eunice High School in the Free State, and Lulama Applegreen of Sol Plaatjie Secondary School in the North West, were the top girl learners in the Platinum and Gold category (written test). They were each awarded a cash prize of R1 000, donated by the Council for Scientific and Industrial Research (CSIR), and Texas Instrument calculators.

All the Gold and Platinum category winners and their teachers received Texas Instruments top-end scientific calculators. Thirteen learners obtained a Distinction Certificate (60–79%) and received Texas Instruments basic scientific calculators.

Professor David Block, Director of the Anglo American Cosmic Dust Laboratory at the University of the Witwatersrand, was the guest speaker. He excited the participating learners with his talk entitled 'The Power of Vision', which was sponsored by Anglogold Ashanti and Metrohm SA.

Concluding his address and urging the learners to espouse a 'change in mindset' and strive for original ideas, Block said: 'Every star is a star, and all beetles are born to scratch.' He added that the imprints of Minquiz 'continue to blaze a most luminous legacy. Truly astronomical!' He also donated four copies of his latest coffee-table book, *Shrouds of the Night*, which he co-authored with fellow astronomer, Professor Kenneth Freeman.

Ms. Zimbini Zwane, Sasol's Community and Government Relations Affairs Manager also addressed the learners. Sasol is an anchor sponsor of Minquiz.

For further information about sponsorship opportunities, contact Garth Williams at: garthw@mintek.co.za or Tel. (011) 709 4476. For general information about Minquiz, please contact Ms Wendy Tshawe at: wendyt@mintek.co.za or Tel. (011) 709 4797. ◆